



## SAR profiles of spirocyclic nicotinamide derived selective HDAC1/HDAC2 inhibitors (SHI-1:2)

Joey L. Methot<sup>a,\*</sup>, Christopher L. Hamblett<sup>a</sup>, Dawn M. Mampreian<sup>a</sup>, Joon Jung<sup>a</sup>, Andreas Harsch<sup>a</sup>, Alexander A. Szewczak<sup>a</sup>, William K. Dahlberg<sup>a</sup>, Richard E. Middleton<sup>a</sup>, Bethany Hughes<sup>a</sup>, Judith C. Fleming<sup>b</sup>, Hongmei Wang<sup>b</sup>, Astrid M. Kral<sup>b</sup>, Nicole Ozerova<sup>b</sup>, Jonathan C. Cruz<sup>c</sup>, Brian Haines<sup>c</sup>, Melissa Chenard<sup>c</sup>, Candia M. Kenific<sup>c</sup>, J. Paul Secrist<sup>b</sup>, Thomas A. Miller<sup>a</sup>

<sup>a</sup> Department of Drug Design and Optimization, Merck Research Laboratories, 33 Avenue Louis Pasteur, Boston, MA 02115, USA

<sup>b</sup> Department of Cancer Biology and Therapeutics, Merck Research Laboratories, 33 Avenue Louis Pasteur, Boston, MA 02115, USA

<sup>c</sup> Department of Oncology Pharmacology, Merck Research Laboratories, 33 Avenue Louis Pasteur, Boston, MA 02115, USA

### ARTICLE INFO

#### Article history:

Received 22 July 2008

Accepted 6 October 2008

Available online 14 October 2008

#### Keywords:

HDAC inhibitor  
Isoform selectivity  
HDAC3  
Internal cavity  
Biaryl  
Spirocycle

### ABSTRACT

A potent family of spirocyclic nicotinyl aminobenzamide selective HDAC1/HDAC2 inhibitors (SHI-1:2) is profiled. The incorporation of a biaryl zinc-binding motif into a nicotinyl scaffold resulted in enhanced potency and selectivity versus HDAC3, but also imparted hERG activity. It was discovered that increasing polar surface area about the spirocycle attenuates this liability. Compound **12** induced a 4-fold increase in acetylated histone H2B in an HCT-116 xenograft model study with acute exposure, and inhibited tumor growth in a 21-day efficacy study with qd dosing.

© 2008 Elsevier Ltd. All rights reserved.

The histone deacetylase (HDAC) family of zinc metalloenzymes play a key role in epigenetic regulation of gene expression.<sup>1</sup> Small molecule HDAC inhibitors<sup>2</sup> have been shown to regulate gene transcription, cell cycle progression, and induce differentiation and/or apoptosis in cancer cells. For example, Zolinza<sup>TM</sup> is a potent HDAC1, 2, 3, 6 inhibitor approved for the treatment of cutaneous manifestations of cutaneous T-cell lymphoma for patients with recurrent disease (Fig. 1).<sup>3</sup>

Unlike HDAC inhibitors having an hydroxamic acid zinc-binding motif, those containing an *ortho*-aminophenyl benzamide inhibit HDACs 1–3 with greater levels of selectivity. We recently reported nicotinyl piperazine **1**<sup>4</sup> which inhibits only HDAC1 (IC<sub>50</sub>: 79 nM), HDAC2 (IC<sub>50</sub>: 308 nM) and HDAC3 (IC<sub>50</sub>: 942 nM). HDACs 1 and 2 share a high degree of homology and are found in the same multi-component nuclear complexes.<sup>5</sup> They are both overexpressed in human cancers and knockdown leads to increased apoptosis in certain cellular contexts.<sup>6</sup> On the other hand, the physiological role of HDAC3 is less well understood. While it is overexpressed in certain colon tumors,<sup>7</sup> HDAC3 is a functional link between the class I and less characterized class IIa HDACs (HDACs 4, 5, 7, 9) that are cata-

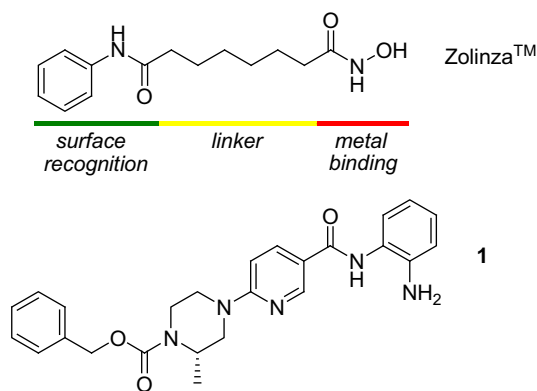


**Figure 1.** Zolinza<sup>TM</sup> the HDAC inhibitor pharmacophore model (upper panel) and *ortho*-aminobenzamide **1** (lower panel).

lytically inactive in the absence of HDAC3.<sup>8</sup> Isoform-selective inhibitors would help further our understanding of the individual roles of the HDAC family, and may offer a potential avenue for improving efficacy and tolerability.<sup>9</sup>

\* Corresponding author. Tel.: +1 617 992 2054; fax: +1 617 992 2403.  
E-mail address: [joey\\_methot@merck.com](mailto:joey_methot@merck.com) (J.L. Methot).

Over the course of optimizing the aminophenyl nicotinamide HDAC inhibitors, we discovered a family of novel spirocyclic compounds typified by structures **2–5** (Table 1). Diazaspirocyclics offer a range of structural diversity and direct appended functionalities and/or hydrophobic groups in orientations unique from piperazines such as **1**. Agents **2–5** possess potent HDAC1 inhibitory activity<sup>10</sup> and HCT-116 colon cancer carcinoma cell antiproliferative activity.<sup>11</sup> However, these compounds did not possess improved selectivity for HDACs 1 and 2 over HDAC3 as compared to **1**. For example, spirocycle **2** is only 7-fold selective for HDAC1 versus HDAC3 (IC<sub>50</sub> 276 nM).

As part of our effort to improve the selectivity of nicotinamides such as **1–5**, we capitalized on the discovery of highly selective hydroxybiphenyl-benzamide **6** from an HTS campaign (Fig. 2).<sup>12</sup> Compound **6** exhibited acceptable potency in HDAC1 and HDAC2 biochemical activity assays (IC<sub>50</sub> 58 and 200 nM, respectively) and was inactive against HDACs 3–8 and HDAC11. In an HCT-116 human colon carcinoma cell viability assay, **6** exhibited modest

antiproliferative activity (GI<sub>50</sub> 2100 nM). The lack of HDAC3 activity exhibited by these biaryl benzamides is in striking contrast to simple benzamides such as **1**. Based on molecular modeling, we believe biaryl benzamides such as **6** extend the pendant aryl ring into the internal cavity of HDAC1/HDAC2.<sup>13</sup>

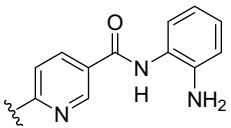
The nicotinamide aniline-containing analogs of **6** are shown in Table 2. *N*-(2-Aminophenyl)nicotinamide **7** was a modest inhibitor of HDAC1 with an IC<sub>50</sub> of 2630 nM. Introduction of a nonpolar aryl group at the 4' position (e.g., **8** and **9**) gave a 100-fold boost in HDAC1 potency and imparted selectivity over HDAC3. However, these modifications enhanced cell-based potency by only 10-fold, with a ~40-fold shift from HDAC1 enzymatic to HCT-116 viability for **8** and **9**.

As anticipated following the SAR developed with nicotinamides such as **1–5**, substitution is most permissive at C(4) of the nicotinamide ring; providing a handle to introduce the surface recognition domain and optimize properties such as solubility, cell permeability and pharmacokinetics. Merging the spirocyclic nicotinamide series with the biaryl motif, we investigated a series of 2,8-diazaspiro[4.5]decanes (Table 3, **10–16**). Nicotinamide **10** exhibited modest activity, with an HDAC1 IC<sub>50</sub> of 160 nM and an HCT-116 growth inhibition GI<sub>50</sub> of 1340 nM. We found that incorporation of the spirocycle enhanced the HDAC1 inhibitory activity of the simpler leads **7–9** by 5- to 10-fold, while >100-fold selectivity versus HDAC3 was maintained for the biaryl analogs. For example, inhibitor **12** inhibited HDAC1 and HDAC2 with IC<sub>50</sub> values of 8 and 44 nM, respectively. The spirocyclic appendage improved cell activity by as much as 25-fold from leads **7–9**, reducing the shift from biochemical to cell activities. Generally the thiophen-2-yl biaryl analogs such as **12** were more potent in the cell proliferation assay than phenyl biaryl inhibitors such as **11**. The former inhibited HCT-116 cell proliferation with a GI<sub>50</sub> of 93 nM.

In line with the proposed mechanism of action, inhibitor **12** induced a 7-fold increase in acetylated histone H3 followed by caspase-3/7 activation and apoptosis in HCT-116 cells at a concentration of 1 μM. In our counterscreen assays, **12** weakly inhibited HDAC8 (IC<sub>50</sub> 6110 nM) but not HDACs 4–7 or HDAC11. The physicochemical properties for this series were also acceptable; solubility and log*D* for compound **12** was 186 μM and 1.45, respectively.

Given the potency of spirocycle **12**, we evaluated its in vivo properties. The pharmacokinetic profiles in rat and dog are listed in Table 4. Intravenous (iv) clearance in rat is moderate (31 ml/min/kg) and bioavailability modest (23%); giving a low normalized oral exposure of 0.3 μM h kg/mg. However, dog PK is more promising with iv clearance 5.9 ml/min/kg and bioavailability quantitative; giving an oral exposure of 8.7 μM h kg/mg. These profiles are in fact very similar to piperazine **1**.<sup>4</sup>

**Table 1**  
Spirocyclic nicotinamide HDAC inhibitors



Compound	HDAC1 IC <sub>50</sub> (nM)	HCT-116 GI <sub>50</sub> (nM)	hERG binding K <sub>i</sub> (nM)
<b>(2)</b>	39	390	>30,000
<b>(3)</b>	120	360	28,500
<b>(4)</b>	130	1920	18,540
<b>(5)</b>	89	400	1760

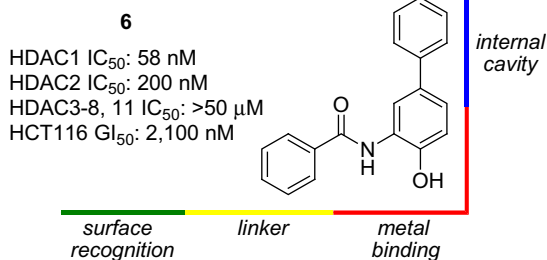
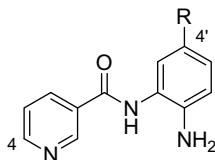


**Figure 2.** A biaryl benzamide imparts >100-fold selectivity for HDACs 1 and 2 versus HDAC3. The new pharmacophore model places the pendant phenyl ring into the internal cavity of histone deacetylase.

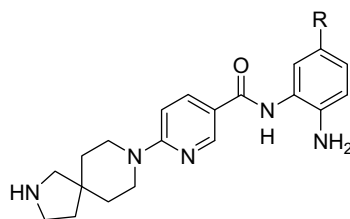
**Table 2**  
Profiles of nicotinyl biaryl leads **7–9**



Compound	HDAC1 IC <sub>50</sub> (nM)	HDAC2 IC <sub>50</sub> (nM)	HDAC3 IC <sub>50</sub> (nM)	HCT-116 GI <sub>50</sub> (nM)
<b>7</b> : R = H	2630	6980	3640	24,200
<b>8</b> : R = phenyl	48	900	11,350	2150
<b>9</b> : R = thiophen-2-yl	65	390	7300	2440

**Table 3**

Variation of the benzamide substitution of a spirocyclic HDAC inhibitor



Compound	HDAC1 IC <sub>50</sub> (nM)	HDAC2 IC <sub>50</sub> (nM)	HDAC3 IC <sub>50</sub> (nM)	HCT-116 GI <sub>50</sub> (nM)	hERG binding K <sub>i</sub> (nM)
<b>10</b> : R = H	160	—	340	1340	21,450
<b>11</b> : R = phenyl	11	110	—	350	590
<b>12</b> : R = thiophen-2-yl	8	44	1260	93	790
<b>13</b> : R = thiophen-3-yl	10	71	1270	140	1210
<b>14</b> : R = <i>N</i> -methylpyrazol-4-yl	36	—	5340	4500	19,250
<b>15</b> : R = pyrazol-3-yl	18	—	5500	>20,000	> 10,000
<b>16</b> : R = <i>N</i> -methylimidazol-4-yl	22	—	>30,000	3490	9800

**Table 4**Pharmacokinetic properties of **12** and **1**

	Rat ( <b>12</b> )	Dog ( <b>12</b> )	Rat ( <b>1</b> )	Dog ( <b>1</b> )
iv dose (mg/kg):	2.0	0.50	2.0	0.90
Clp (ml/min/kg):	31	5.9	52	7.4
V <sub>dss</sub> (L/kg):	8.6	3.3	2.1	2.1
t <sub>1/2</sub> (h):	6.2	6.7	0.93	5.6
po dose (mg/kg):	4.0	1.0	4.0	1.8
AUCN				
(μM h kg/mg):	0.28	8.7	0.23	3.8
F (%):	23	100	37	73

A xenograft model of CD-1 nude mice bearing a tumor consisting of a HCT-116 colon carcinoma cell line was used to evaluate the in vivo antitumor potential of our HDAC inhibitors. Acute intraperitoneal (ip) administration of **12** (50 mg/kg) caused a marked >4-fold increase in tumor acetylated histone H2B. Compound **12** was administered once daily ip over a 21-day period (Fig. 3) at 10, 15 and 20 mg/kg (12 mice per dose group). The mice tolerated the 10 and 15 mg/kg studies (less than 5% body weight loss), but not the 20 mg/kg study which was terminated early. The 10 and 15 mg/kg groups gave a 49% and 74% tumor growth inhibition, respectively. Average plasma levels of **12** in the 15 mg/kg dose group were 3.4, 0.32, 0.05 and 0.03 μM at 6, 24, 48 and 72 h, respectively. The oral bioavailability of **12** in mice permitted a xenograft efficacy study with once-daily oral administration. Following 150 mg/kg for 21 days, a 50% tumor growth inhibition was achieved. With 300 mg/kg oral dosage, a 70% growth inhibition was observed. Average plasma levels were 11 and 0.22 μM at 6 and 24 h timepoints for the 150 mg/kg group, while the 300 mg/kg group averaged 21 and 0.78 μM plasma levels at 6 and 24 h. For both oral doses, the mice experienced low body weight loss.

Unfortunately, inhibitors **11–13** were also modest binders of the hERG-encoded potassium ion channel. Inhibition of the hERG ion channel resulting in inhibition of the rapid component of the delayed rectifier potassium current (*I<sub>Kr</sub>*) has been implicated in QT interval prolongation and life-threatening cardiac arrhythmia.<sup>14</sup> A displacement assay using a known radiolabeled methanesulfonanilide hERG binder, MK-499,<sup>15</sup> was used to screen for hERG affinity.<sup>16</sup> In this binding assay, hERG *K<sub>i</sub>* values for phenyl and thiophene biaryl analogs **11–13** ranged from 590 to 1210 nM. Thio-

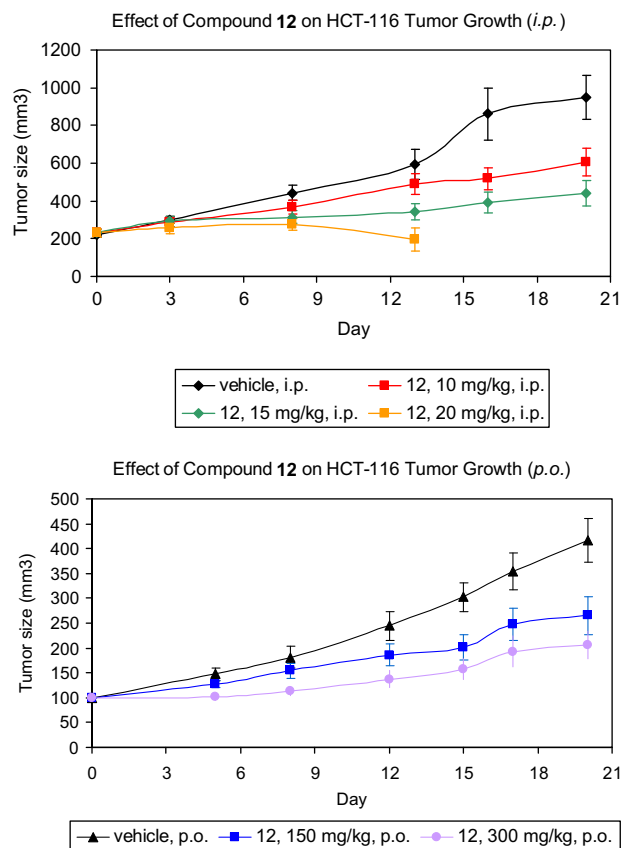


**Figure 3.** 21-Day efficacy study of compound **12** in a HCT-116 colon carcinoma mouse xenograft model via ip administration (top graph) and po administration (bottom graph).

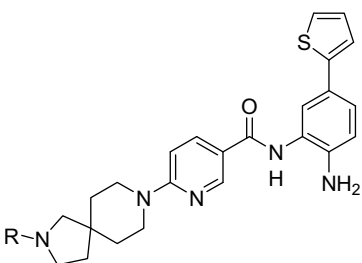
phen-2-yl biaryl **12** was weakly active in a patch clamp assay with chinese hamster ovary cells expressing human hERG channel, inhibiting with an EC<sub>50</sub> of 10,000 nM. Given the weaker activity in the functional assay, we proceeded to evaluate the potential cardiovascular liability of **12** in an anaesthetized CV dog with an acute iv dose escalation. While no effect was observed up to 3 mg/kg reaching a plasma concentration of 6 μM, ECG monitoring indi-

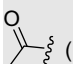
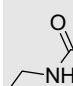
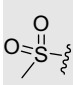
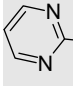
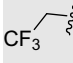
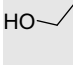
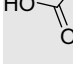
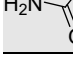
cated an 8% increase in the QT interval at 10 mg/kg reaching 30  $\mu$ M plasma level. The observed QT prolongation in vivo was likely the result of hERG binding affinity despite the 10-fold shift in cell functional activity.

The hERG-encoded ion channel consists of four subunits each consisting of six transmembrane helices that together form a pore which closes upon binding to substrates, entrapping them. Key binding residues include Phe656 and Tyr652 that have been implicated in  $\pi$ – $\pi$  or cation– $\pi$  interactions as well as Thr623 and Ser624 that are capable of hydrogen-bond networks.<sup>17</sup> Val625, Gly648 and Val659 have also been implicated in drug binding. The importance and promiscuity of the ion channel has led to the development of a variety pharmacophore models for substrate binding.<sup>18</sup>

In an attempt to negate the hERG binding affinity of **12** by reducing the overall hydrophobicity we introduced polar functionalities into the molecule. Hence more polar pyrazolyl and imidazolyl biaryl analogs **14**–**16** were prepared. These modifications afforded compounds active in the HDAC1 biochemical assay ( $IC_{50}$  18–36 nM) with significantly diminished hERG affinity. However, they had significantly reduced HCT-116 antiproliferative activity ( $GI_{50}$  3490  $\rightarrow$  20,000 nM); likely the result of poor cell permeability.

**Table 5**  
Attenuation of spirocycle amine basicity of **12**

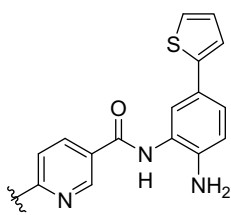


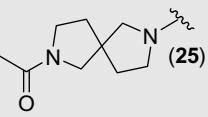
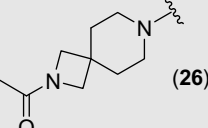
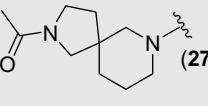
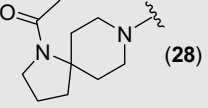
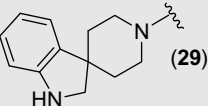
Substituent R	HDAC1 $IC_{50}$ (nM)	HCT-116 $GI_{50}$ (nM)	hERG binding $K_i$ (nM)	hERG functional $EC_{50}$ (nM)
H ( <b>12</b> )	8	93	790	10,000
 ( <b>17</b> )	9	160	9790	10,100
 ( <b>18</b> )	14	180	460	5000
 ( <b>19</b> )	8	260	5210	3300
 ( <b>20</b> )	28	520	760	3350
 ( <b>21</b> )	17	740	1900	
 ( <b>22</b> )	6	65	170	6500
 ( <b>23</b> )	17	>20,000	3200	
 ( <b>24</b> )	13	97	97	

The location of a basic amine in close proximity ( $\sim$ 2–5 atoms) to an aromatic system is a well-established pharmacophore for inhibition of the hERG ion channel.<sup>19</sup> Hence electronically deactivating groups were attached to the terminal nitrogen atom of the spirocycle, while keeping the thiophen-2-yl biaryl constant (Table 5). Amides such as acetamide **17** maintained good potency in the HDAC1 biochemical and HCT-116 antiproliferation assays. Furthermore the in vitro hERG binding affinity ( $K_i$  9790 nM) of **17** was significantly reduced from **12**. Unfortunately acetamide **17** (and related substituted amides) were as active as **12** in the functional patch clamp assay with an  $EC_{50}$  of 10,100 nM. An additional concern was the potential for metabolic hydrolysis of the amide giving **12** in vivo; a potent hERG binding agent. Ureas and sulfonamides such as **18** and **19** as well as pyrimidin-2-yl analog **20** were potent in both HDAC1 and HCT-116 assays but retained activity in the hERG binding assay. Several other electronically deactivating groups such as 2,2,2-trifluoroethyl, hydroxyethyl, acetic acid and acetamide analogs **21**–**24** were prepared to attenuate the basicity of the amine. However these also failed to attenuate the hERG activity of this spirocycle. As expected, acid **23** lacked cell activity.

Several other spirocyclic designs derived from commercially available precursors were investigated to address the problem of hERG affinity. Racemic 2,7-diazaspiro[4.4]nonane was found to be an equipotent alternative spirocycle and several analogs were

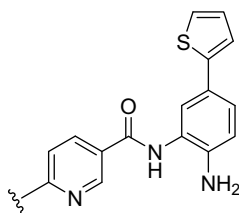
**Table 6**  
Alternative spirocyclic designs



Compound	HDAC1 $IC_{50}$ (nM)	HCT-116 $GI_{50}$ (nM)	hERG binding $K_i$ (nM)	hERG functional $EC_{50}$ (nM)
 ( <b>25</b> )	12	130	2790	10,300
 ( <b>26</b> )	23	390	6300	10,100
 ( <b>27</b> )	8	260	3810	10,000
 ( <b>28</b> )	23	470	16,740	N/A
 ( <b>29</b> )	230	2030	10,250	N/A

prepared as exemplified by **25** (Table 6). Biochemical and cell-based activities were acceptable but again these spirocycles were hERG-active in both the binding and functional assays. Others such

**Table 7**  
Increased spirocycle polar surface area



Compound		HDAC1	HCT-116	hERG binding
		IC <sub>50</sub> (nM)	GI <sub>50</sub> (nM)	K <sub>i</sub> (nM)
<b>30</b>		13	340	>10,000
<b>31</b>		29	280	9420
<b>32</b>		21	190	8620 <sup>a</sup>
<b>33</b>		11	49	10,980
<b>34</b>		13	51	8699
<b>35</b>		16	430	9070
<b>36</b>		11	110	7540
<b>37</b>		27	330	6330
<b>38</b>		7	320	14,560
<b>39</b>		8	250	>10,000 <sup>b</sup>

<sup>a</sup> hERG functional EC<sub>50</sub> 18,000 nM.

<sup>b</sup> hERG functional EC<sub>50</sub> >30,000 nM.

**Table 8**  
Pharmacokinetic properties of **39**

	Rat	Dog
iv dose (mg/kg):	2.0	0.50
Clp (ml/min/kg):	7.4	9.8
V <sub>dss</sub> (L/kg):	0.47	2.3
04 (h):	2.6	6.8
po dose (mg/kg):	4.0	1.0
AUCN		
μM h kg/mg):	0.75	0.65
F (%):	13	18

as 6–4' and 6–5' spirocycles exemplified by **26**, **27** and **28** exhibited very similar SAR with respect to HDAC1 and HCT-116 activity as well as hERG affinity. Another consideration was to attenuate the spirocyclic amine basicity through fusion of a third aryl ring, however in most cases these compounds had diminished HDAC1 activity without improved selectivity versus hERG. For example, indolyl piperidinyl spirocycle **29** was one log unit less potent than related inhibitor **12**.

Next we altered the spirocyclic design to incorporate increased polar surface area within the spirocycle itself (Table 7). For example, spirocyclic ketone **30** maintained good HDAC1 and HCT-116 viability activities and was inactive in the hERG binding assay. However, the hERG affinity returned with alcohol **31**; a potential metabolite of ketone **30**. Lactams **32**, **33** and **34** had good to excellent HDAC1 and HCT-116 activities and comparable hERG binding affinity. However, lactam **32** was weakly active in the hERG cell functional assay (18,000 nM). Despite a reasonable exposure in the mouse PD assay following oral administration (150 mg/kg po; C<sub>max</sub> 34 μM, AUC 88 μM h), **32** induced a marginally-significant 2-fold increase in acetylated histone H2B. Potent lactam **34** also failed in mouse PD.

Alternative designs investigated include hydantoin **35** and amino lactams **36** and **37**, which inhibited the ion channel, albeit weakly. Two promising candidates were cyclic urea **38** and carbamate **39**: both potent in the HDAC1 biochemical (IC<sub>50</sub> 7 and 8 nM, respectively) and HCT-116 proliferation assays. Low hERG binding affinities were promising for both (K<sub>i</sub> values of 14,560 and >10,000 nM); and **39** was also inactive in the hERG cell functional activity assay (EC<sub>50</sub> >30,000 nM). Unfortunately, both **38** and **39** failed to increase acetylated histone H2B when administered orally in our mouse PD model, presumably due to insufficient exposure.<sup>20</sup> However, compound **39** did induce histone acetylation when administered ip (150 mg/kg ip; 4-fold increase in Ac-H2B/H2B). Consistent with our experience in mouse, **39** also had low rat and dog bioavailability (Table 8).

While increasing polar surface area to over 100 Å<sup>2</sup> gave a high probability of mitigating hERG, it is also noteworthy that numerous compounds with PSA >110 Å<sup>2</sup> did, in fact, bind to the ion channel. Attempts to correlate hERG affinity to logP or logD were also unsuccessful, as were attempts with other physicochemical descriptors. In addition, docking studies based on the homology model of hERG channel were carried out, but a correlation between docking scores and binding affinity was not observed.<sup>21</sup> However, it should be noted that further analysis entailing the flexibility of the channel was not explored.<sup>22</sup>

In summary, spirocyclic nicotinamides are potent alternatives to our earlier reported piperazine nicotinamides such as **1**.<sup>4</sup> The incorporation of a nonpolar biaryl zinc-binding motif derived from HTS leads<sup>12b</sup> enhanced potency and rendered the inhibitors >500-fold selective for HDACs 1 and 2 over HDAC3. Inhibitor **12** is a scalable,<sup>23</sup> potent and selective SHI-1:2 with antitumor activity in an HCT-116 human colon carcinoma mouse xenograft model study. However, hERG affinity has limited the further development of



**12.** Efforts to identify a safe, orally efficacious alternative to **12** will be the subject of future communications.

## References and notes

- Lund, A. H.; Van Lohuizen, M. *Genes Dev.* **2004**, *18*, 2315.
- (a) Miller, T. A.; Witter, D. J.; Belvedere, S. J. *Med. Chem.* **2003**, *46*, 5097; (b) Paris, M.; Porcelloni, M.; Binaschi, M.; Fattori, D. J. *Med. Chem.* **2008**, *51*, 1505.
- (a) Richon, V. M. *Br. J. Cancer* **2006**, *95*, S2; (b) O'Connor, O. A. *Br. J. Cancer* **2006**, *95*, S7; (c) Duvic, M.; Zhang, C. *Br. J. Cancer* **2006**, *95*, S13; (d) Marks, P. A.; Breslow, R. *Nat. Biotechnol.* **2007**, *25*, 84.
- Hamblett, C. L.; Methot, J. L.; Mampreian, D. M.; Sloman, D. L.; Stanton, M. G.; Kral, A. M.; Fleming, J. C.; Cruz, J. C.; Chenard, M.; Ozerova, N.; Hitz, A. M.; Wang, H.; Deshmukh, S. V.; Nazef, N.; Harsch, A.; Hughes, B.; Dahlberg, W. K.; Szewczak, A. A.; Middleton, R. E.; Mosley, R. T.; Secrist, J. P.; Miller, T. A. *Bioorg. Med. Chem. Lett.* **2007**, *17*, 5300.
- Knoepfler, P. S.; Eisenman, R. N. *Cell* **1999**, *99*, 447.
- (a) Laguer, G.; O'Carroll, D.; Rembold, M.; Khier, H.; Tischler, J.; Weitzer, G. *EMBO J.* **2002**, *21*, 2672; (b) Huang, B. H.; Laban, M.; Leung, C. H.; Lee, L.; Lee, C. K.; Salto-Tellez, M. *Cell Death Differ.* **2005**, *12*, 395; (c) Weihert, W.; Roske, A.; Gekeler, V.; Beckers, T.; Stephan, C.; Jung, K.; Fritzsche, F. R.; Niesporek, S.; Denkert, C.; Dietel, M.; Kristiansen, G. *Br. J. Cancer* **2008**, *98*, 604.
- (a) Wilson, A. J.; Byun, D.-S.; Popova, N.; Murray, L. B.; L'Italien, K.; Sowa, Y.; Arango, D.; Velcich, A.; Augenlicht, L. H.; Mariadason, J. M. *J. Biol. Chem.* **2006**, *281*, 13548; (b) Weichert, W.; Roske, A.; Niesporek, S.; Noske, A.; Buckendahl, A.-C.; Dietel, M.; Gekeler, V.; Boehm, M.; Beckers, T.; Denkert, C. *Clin. Cancer Res.* **2008**, *14*, 1669.
- (a) Grozinger, C. M.; Hassig, C. A.; Schreiber, S. L. *Proc. Natl. Acad. Sci. U.S.A.* **1999**, *96*, 4868; (b) Fischle, W.; Dequiedt, F.; Fillion, M.; Hendzel, M. J.; Voelter, W.; Verdine, E. J. *Biol. Chem.* **2001**, *276*, 35826.
- Karagiannis, T. C.; El-Osta, A. *Leukemia* **2007**, *21*, 61.
- For enzyme assay procedure, see Ref. 4.
- For cell viability assay procedure, see Ref. 4.
- (a) Witter, D. J.; Harrington, P.; Wilson, K. J.; Fleming, J. C.; Kral, A. M.; Secrist, J. P.; Miller, T. A. *Bioorg. Med. Chem. Lett.* **2008**, *18*, 726; (b) Methot, J. L.; Chakravarty, P. K.; Chenard, M.; Close, J.; Cruz, J. C.; Dahlberg, W. K.; Fleming, J.; Hamblett, C. L.; Hamill, J. E.; Harrington, P.; Harsch, A.; Heidebrecht, R.; Hughes, B.; Jung, J.; Kenific, C. M.; Kral, A. M.; Meinke, P. T.; Middleton, R. E.; Ozerova, N.; Sloman, D. L.; Stanton, M. G.; Szewczak, A. A.; Tyagarajan, S.; Witter, D. J.; Secrist, J. P.; Miller, T. A. *Bioorg. Med. Chem. Lett.* **2008**, *18*, 973; (c) Moradei, O. M.; Mallais, T. C.; Frechette, S.; Paquin, I.; Tessier, P. E.; Leit, S. M.; Fournel, M.; Bonfils, C.; Trachy-Bourget, M.-C.; Liu, J.; Yan, T. P.; Lu, A.-H.; Rahil, J.; Wang, J.; Lefebvre, S.; Li, Z.; Vaisburg, A. F.; Besterman, J. M. *J. Med. Chem.* **2007**, *50*, 5543.
- Wang, D.-F.; Wiest, O.; Helquist, P.; Lan-Hargest, H.-Y.; Wiech, N. L. *J. Med. Chem.* **2004**, *47*, 3409.
- (a) Sanguinetti, M. C.; Mitcheson, J. S. *Trends Pharm. Sci.* **2005**, *26*, 119; (b) Aronov, A. M. *Drug Discov. Today* **2005**, *10*, 149.
- Lynch, J. J., Jr.; Wallace, A. A.; Stupienski, R. F., III; Baskin, E. P.; Beare, C. M.; Appleby, S. D.; Salata, J. J.; Jurkiewicz, N. K.; Sanguinetti, M. C.; Stein, R. B.; Gehret, J. R.; Kothstein, T.; Claremon, D. A.; Elliott, J. M.; Butcher, J. W.; Remy, D. C.; Baldwin, J. J. *J. Pharmacol. Exp. Ther.* **1994**, *269*, 541.
- The hERG  $K_i$  values were determined through binding competition experiments using membrane preparations from human embryonic kidney (HEK293) cells that constitutively express hERG.
- (a) Mitcheson, J. S.; Perry, M. D. *Curr. Opin. Drug Discov. Devel.* **2003**, *6*, 667; (b) Stansfield, P. J.; Sutcliffe, M. J.; Mitcheson, J. S. *Expert Opin. Drug Metab. Toxicol.* **2006**, *2*, 81.
- (a) Fernandez, D.; Ghanta, A.; Kauffman, G. W.; Sanguinetti, M. C. *J. Biol. Chem.* **2004**, *279*, 10120; (b) Jamieson, C.; Moir, E. M.; Rankovic, Z.; Wishart, G. J. *Med. Chem.* **2006**, *49*, 5029; (c) Waring, M. J.; Johnstone, C. *Bioorg. Med. Chem. Lett.* **2007**, *17*, 1759.
- Choe, H.; Nah, K. H.; Lee, S. N.; Lee, H. S.; Lee, H. S.; Jo, S. H.; Leem, C. H.; Jang, Y. J. *Biochem. Biophys. Res. Commun.* **2006**, *344*, 72.
- Compounds **38** and **39** were dosed at 150 mg/kg po. Exposure for **38**: AUC 10  $\mu\text{M h}$ ,  $C_{\text{max}}$  2  $\mu\text{M}$ . Exposure for **39**: AUC 14  $\mu\text{M h}$ ,  $C_{\text{max}}$  6  $\mu\text{M}$ .
- Farid, R.; Day, T.; Friesner, R. A.; Pearlstein, R. A. *Bioorg. Med. Chem.* **2006**, *14*, 3160.
- Rajamani, R.; Tounge, B. A.; Li, J.; Reynolds, C. H. *Boorg. Med. Chem. Lett.* **2005**, *15*, 1737.
- For a synthesis of **12**, see: Berk, S. C.; Close, J.; Hamblett, C.; Heidebrecht, R. W.; Kattar, S. D.; Kliman, L. T.; Mampreian, D. M.; Methot, J. L.; Miller, T.; Sloman, D. L.; Stanton, M. G.; Tempest, P.; Zabierek, A. A. *Spirocyclic compounds as HDAC inhibitors*. WO 2007/061978.